Received: 2 March 2017
DOI: 10.1002/mop.30777

Design of high return loss logarithmic spiral antenna

Leonardo Morbidel[1,2] | **Laureano A. Bulus Rossini**[1,3] | **Pablo A. Costanzo Caso**[1,3]

[1] Instituto Balseiro (CNEA-UNCuyo), Av. Bustillo 9500, Bariloche, RN 1900, Argentina

[2] CNEA Centro Atómico Bariloche, Bariloche, RN, Argentina

[3] CONICET CCT Patagonia Norte, Bariloche, RN, Argentina

Correspondence
Leonardo Morbidel, Instituto Balseiro (CNEA-UNCuyo), Av. Bustillo 9500, Bariloche, RN 1900, Argentina.
Email: leomorbidel@ib.edu.ar

Abstract

We propose a new strategy for designing a logarithmic spiral antenna and the impedance adapter to operate in a frequency range of 1 to 10 GHz. Numerical and experimental results show a decrease in return loss being higher than 20 dB in almost the entire range of operation.

KEYWORDS

frequency independent antenna, impedance matching, logarithmic spiral antenna, microstrip to parallel striplines balun

1 | INTRODUCTION

Frequency independent antennas were proposed by Rumsey in 1957[1] and have been widely used in communications and radar systems because of their good performance in high bandwidth systems.[2–4] A particular case belonging to this group are the logarithmic spiral antennas, which, due to their balanced structure, need to be fed by means of a balun (ie, the a device transforming a balanced to an unbalanced system). In addition, it is possible to set the antenna design parameters in order to obtain a self-complementary geometry, which yields a constant impedance value.[5]

To achieve optimum performance of the complete antenna, the two concepts mentioned above (balun and impedance matching) must be verified in the whole bandwidth in which the system operates. Several designs have been proposed based on coplanar waveguides.[6–8] These designs have a return loss of about 10 dB, and only over a limited bandwidth. Another variant, such as microstrip line to parallel stripline, allows to increase the spectral range of work,[9–12] but does not establish a specific criterion to determine the impedance at the balanced end, and do not consider the effect of having a finite ground plane, instead of an infinite one at the unbalanced side.

In this work, we present the design of a logarithmic spiral antenna operating in a 1–10 GHz bandwidth for UWB applications.[13–15] As part of the antenna design, an impedance matching network is developed, based on the microstrip to parallel stripline conversion. A new method is considered in order to calculate the dimensions of the balanced end of the adapter.[16] This allows achieving a considerably high return loss, maintaining the performance of the antenna within the specified spectral range.

The paper is structured as follows: in Section 2 the design of the antenna is presented, while in Section 3 the matching network design is introduced according to the obtained results of the characterization of the antenna. In Section 4 numerical simulations are compared with the experimental results obtained from the adapter-antenna system. Finally, the conclusions are presented in Section 5.

2 | ANTENNA DESIGN

The logarithmic spiral antenna consists of two symmetric arms which are fed at their origin, as shown in Figure 1A. Each arm is described by the following expressions in polar coordinates: $r_1(\phi) = r_0\exp(\alpha\phi)$ and $r_2(\phi) = r_0\exp[\alpha(\phi-\delta)]$, where r_0 is the initial radius, α is the growth rate of the spirals, which is related to the number of turns of each arm, and δ is the phase shift between two consecutive curves.

The design parameters are determined taking into account the principle of radiation for this kind of antennas, which establishes that the radiated electric field is present on circumferences of length equal to λ, being λ the corresponding wavelength at the operation frequency.[17] In this way, the dimensions for the internal and external radius are obtained, depending on the required working bandwidth from the following expressions: $R_{int} = r_2(0) \leq c/2\pi f_{max}$ and $R_{ext} = r_1(\varphi_f) \geq c/2\pi f_{min}$, where φ_f is the maximum reached angle by the spiral arms and are defined as $\varphi_f = 2\pi N$, where N is the number of turns of each arm.

The proposed design was fabricated using a substrate of type RT-duroid 5880 with a relative dielectric constant $\varepsilon_r = 2.2$, as shown in Figure 1B. The obtained dimensions are $R_{int} = 3$ mm and $R_{ext} = 60$ mm, for values of $\alpha = 0.1$ rad^{-1} and phase $\delta = \pi/2$ rad, this last parameter allows to obtain a self-complementary geometry.

Spiral antennas exhibit excellent performance in broadband systems. However, in order to achieve such

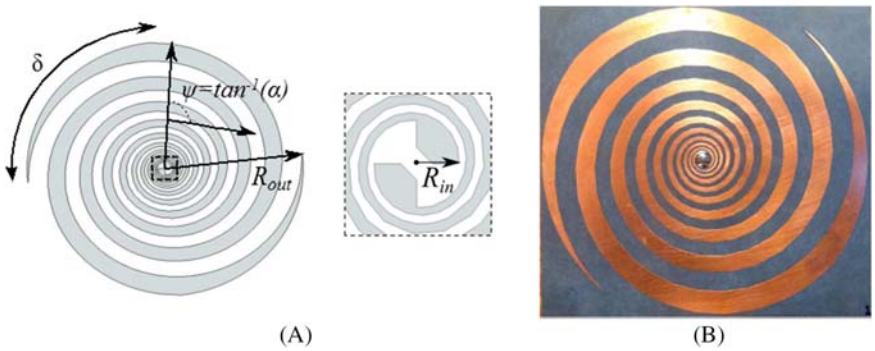

FIGURE 1 (A) Logarithmic spiral antenna with the parameters that define its geometry and (B) fabricated prototype. [Color figure can be viewed at wileyonlinelibrary.com]

performance, it is necessary that the matching network is implemented in a way that does not degrade the behavior of the designed antenna. Thus, one of the important points for the design of the feeder is to determine the proper impedance of the antenna. Although the impedance of a self-complementary structure of infinite dimensions is analyzed in reference,[5] the requirement for realizing a bounded antenna that can be implemented produces changes in the characteristic impedance and other parameters. Figure 2A shows the numerical results corresponding to the impedance of the antenna, both in its real and imaginary part. Two regions can be clearly identified from which the working bandwidth is defined. In the region of low frequencies, the impedance is dominated by a series of resonant peaks, whose effect is due to the external truncation of the antenna, while the remaining region has an approximately constant behavior, which allows approximating a fixed value for Z_{in}, with which the balun is designed.

Since the impedance of the antenna does not present a constant value due to the truncation and other causes related to the implementation, it is necessary to analyze carefully how to match its impedance. In this way, it was proposed to study under what matching conditions in the feeding region the highest return loss is obtained. To do that, the reflection coefficient was analyzed for different generator impedances considered as connected to the spiral arms. The chosen magnitudes correspond to the minimum, mean and maximum values of the real part obtained from Figure 2A, given by Z_{port} = 100, 130 y 180 Ω, respectively. Figure 2B shows the corresponding reflection coefficient for the three mentioned cases. It can be observed that for frequencies below 7.5 GHz, the best matching condition is achieved by connecting a generator whose impedance is Z_{port} = 130 Ω, reaching a return loss higher than 20 dB for frequencies below 4 GHz, and higher than 14 dB in the whole operation range.

Now that the best matching condition is defined, the antenna feeder must be designed by taking into account that its output characteristic impedance is not constant over the frequency range of operation, and that the designed antenna has a balanced input impedance.

3 | ADAPTER DESIGN

To design the adapter two issues were addressed. The first is the matching of impedance values because devices and instruments employed in microwave have usually 50 Ω impedances, while the designed antenna must be fed with 130 Ω to achieve maximum return loss. The second issue is the development of a balun that allows the transformation between balanced and unbalanced systems.

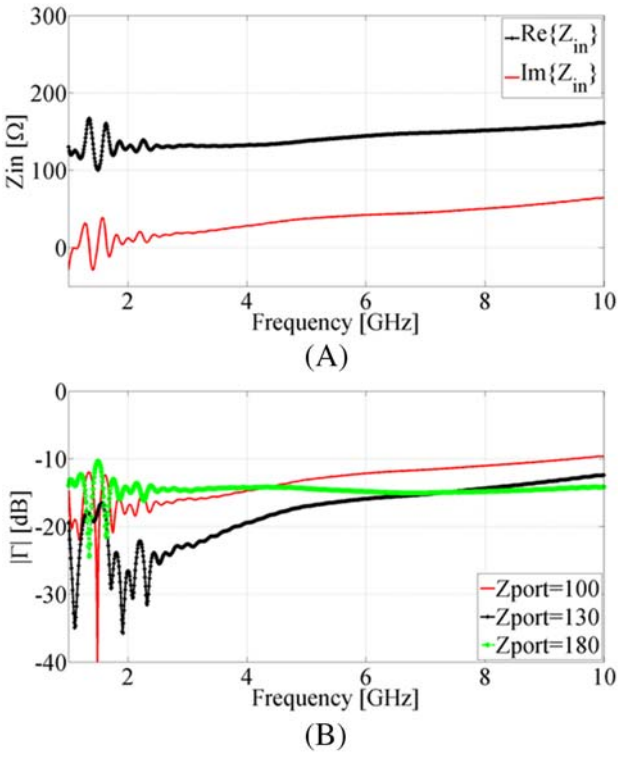

FIGURE 2 (A) Real and imaginary part of the impedance of the antenna and (B) reflection coefficient for three different matching conditions: 100 Ω, 130 Ω, and 180 Ω. [Color figure can be viewed at wileyonlinelibrary.com]

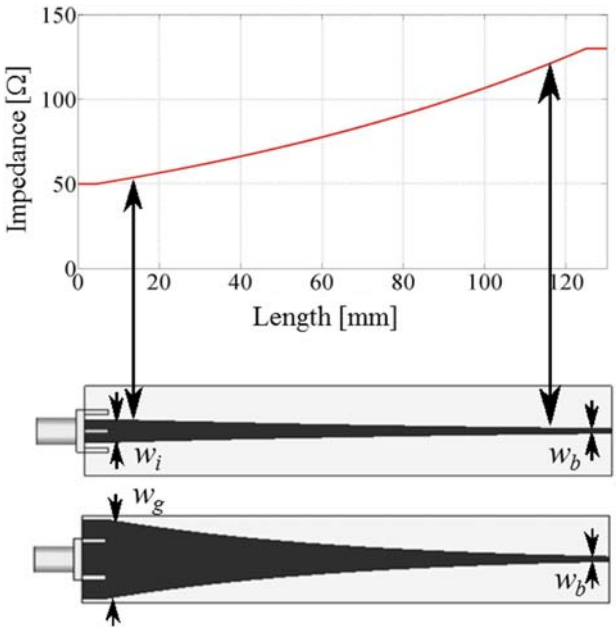

FIGURE 3 Proposed scheme for the balun/impedance adapter. The design has an exponential distribution in the impedance value with a progressive variation of both the main conductor and the ground plane. [Color figure can be viewed at wileyonlinelibrary.com]

The proposed impedance matching technique is based on a microstrip taper. This kind of microstrip line is usually used as an impedance adapter, however, if a similar progressive variation is applied to the ground side, a combined balun/impedance adapter is simultaneously obtained.

The modification of the width is performed following a distribution of the impedance along the line as shown in Figure 3. There are different mathematical functions to implement this distribution and knowing these expressions it is possible to obtain the reflection coefficient of the adapter.[18] In this paper, we propose to use an exponential distribution and analyze the effect caused by the use of a finite ground plane, which the specific literature has not addressed. In this way, an expression of Γ can be obtained for an exponential distribution given by:

$$\Gamma(\omega)=\frac{1}{2L}\ln\left(\frac{Z_L(\omega)}{Z_0}\right)\int_0^L e^{-j2\beta(\omega,l)l}\mathrm{d}l, \tag{1}$$

where $Z_L(\omega)$ is the input impedance of the antenna, Z_0 is the impedance of the generator, L is the length of the adapter,

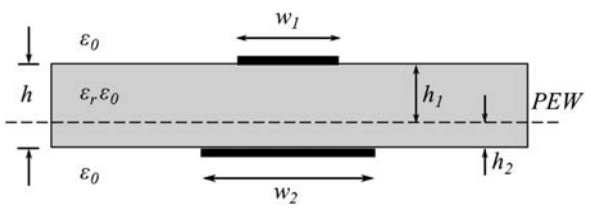

FIGURE 4 Two parallel lines with an infinite perfect electric wall (PEW)

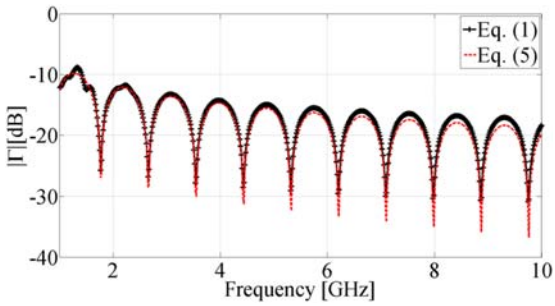

FIGURE 5 Module of the reflection coefficient obtained for the two models, with a length $L = 0.125$ mm on a substrate of thickness $h = 1.5748$ mm and a permittivity $\varepsilon_r = 2.2$. [Color figure can be viewed at wileyonlinelibrary.com]

and β is the propagation constant, which depends on both the frequency and the position along the adapter and is defined as:

$$\beta(\omega,l)=\frac{\omega}{C}\sqrt{\varepsilon_{\mathrm{eff}}(l)}, \tag{2}$$

being $\varepsilon_{\mathrm{eff}}$ the effective dielectric constant which depends on the thickness of the substrate h and the width of the conductor line along of the adapter, in the following manner:

$$\varepsilon_{\mathrm{eff}}=\frac{\varepsilon_r+1}{2}+\frac{\varepsilon_r-1}{2}\frac{1}{\sqrt{1+12\left(h/w\right)}}. \tag{3}$$

Although several works that propose the design of this type of adapters can be found, they do not present a detailed description of the calculation of the width of a conducting line when the ground plane is finite. On the other hand, in the presented designs in references[11] and Ref. [12] the return loss do not exceed 15 dB in a similar operating frequency range. A way of analyzing the impedance of two parallel lines is developed in reference[16] where it is proposed the existence of a perfect electric wall (PEW) between both lines, separated a distance h_1 and h_2 from each one. In this way, the problem of two balanced lines is transformed in two independent microstrip problems. Figure 4 shows a cut of the microstrip line with finite ground plane where the model parameters h_1 and h_2 are shown.

The position where the ideal ground plane is located with respect to the upper conducting line as a function of the widths of the parallel lines (w_1 and w_2) and the substrate thickness h, is calculated as

$$h_1=\frac{h}{2}+\frac{h}{2}\frac{\left(w_2/w_1\right)^{w_1/h}-1}{\left(w_2/w_1\right)^{w_1/h}+1}. \tag{4}$$

To determine the width of the microstrip line at the unbalanced end it is assumed $w_2 \gg w_1$. In this way, it is possible to consider w_2 as an infinite ground plane so that $h_1 = h$ in Equation 4. Therefore, it is required to obtain the value

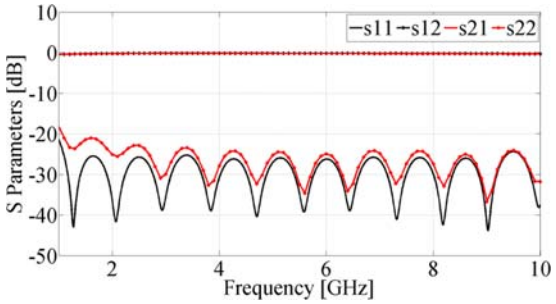

FIGURE 6 Simulation of the S parameters for the two port balun/impedance adapter for a 50 Ω unbalanced load and for a 130 Ω balanced load. [Color figure can be viewed at wileyonlinelibrary.com]

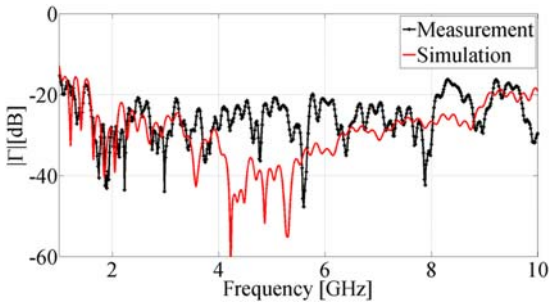

FIGURE 8 Comparison of the measured and simulated reflection coefficient of the matched antenna. [Color figure can be viewed at wileyonlinelibrary.com]

of w_1 that fulfill $Z_0(w_1,h) = 50\ \Omega$. On the other hand, for the balanced end it is verified that $w_1 = w_2 = w_b$, and then $h_1 = h_2 = h/2$. Therefore the impedance in that region is $Z_{port} = Z_0(w_1,h_1) + Z_0(w_2,h_2) = 2Z_0(w_b,h/2) = 130\ \Omega$.

In order to determine the length of the adapter, an approximation was made in Equation 1 where it was considered that the propagation constant does not depend on the position along the adapter line, ie, $\beta(\omega,l) = \beta(\omega)$, that yields a reflection coefficient of the form

$$\Gamma(\omega) = \frac{1}{2}\ln\left(\frac{Z_{port}}{Z_0}\right)\frac{\text{sen}(\beta L)}{\beta L}e^{-j\beta L}. \quad (5)$$

By using Equation 5 and setting values of $|\Gamma| < 10$ dB the minimum length of the adapter that satisfies this condition is obtained as $L > 120$ mm. The values obtained for the adapter are $w_i = 5$ mm and $w_g = 18$ mm for the unbalanced part of the network, while $w_b = 1.6$ mm for the balanced end and a total length $L = 125$ mm, using a substrate of type RT-duroid 5880 with a relative dielectric constant $\varepsilon_r = 2.2$.

Finally, it is necessary to know how significant the error introduced by the approximation $\beta(\omega,l) = \beta(\omega)$ is. In order to do that Figure 5 shows the modulus of the reflection coefficient for the numerical integration of Equation 1 and the analytic expression of Equation 5. It is evident the similarity between the two curves, being the difference less than 0.5 dB in the considered frequency range. This result allows to validate the approximation employed in Equation 5 and to perform the design using that expression since the level of complexity is considerably reduced.

Once the parameters of the impedance adapter are defined, the corresponding simulations were done to analyze the performance. The results obtained are observed in Figure 6, where the S (or scattering) parameters are shown, considering the adapter as a two-port network connected to a 50 Ω input and a 130 Ω output. The transfer parameters, S_{21} and S_{12}, are approximately 0 dB and account for the low transmission loss. While the reflection parameters, S_{11} and S_{22}, show a return loss greater than 20 dB in the specified bandwidth. In addition, it can be verified that the response that presents the coefficients S_{11} agrees with the expression obtained in Equation 5 and shown in Figure 5.

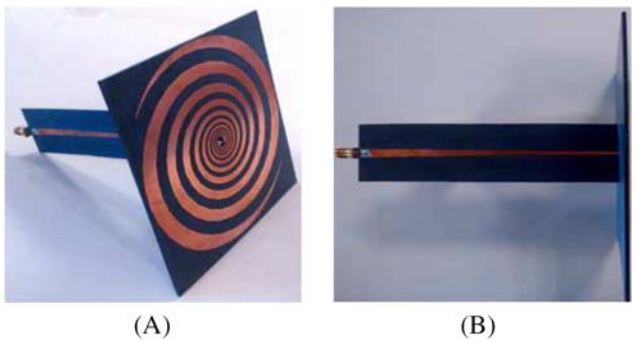

FIGURE 7 Fabricated prototype of the logarithmic spiral antenna and balun/impedance adapter. [Color figure can be viewed at wileyonlinelibrary.com]

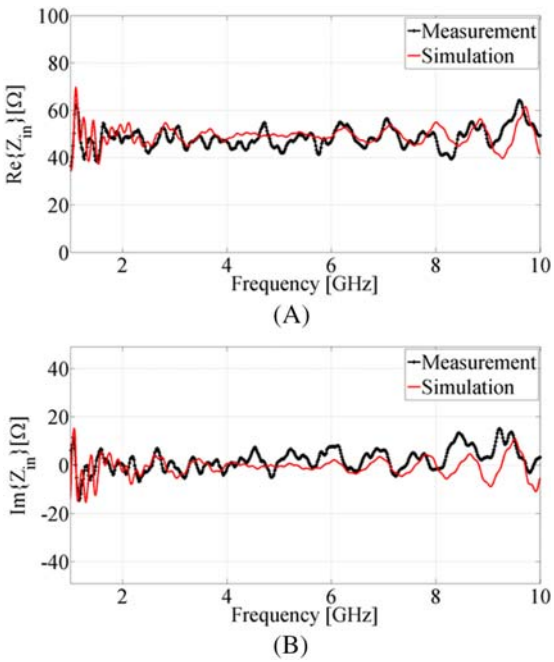

FIGURE 9 (A) Real and (B) imaginary parts of the proper impedance of the antenna. [Color figure can be viewed at wileyonlinelibrary.com]

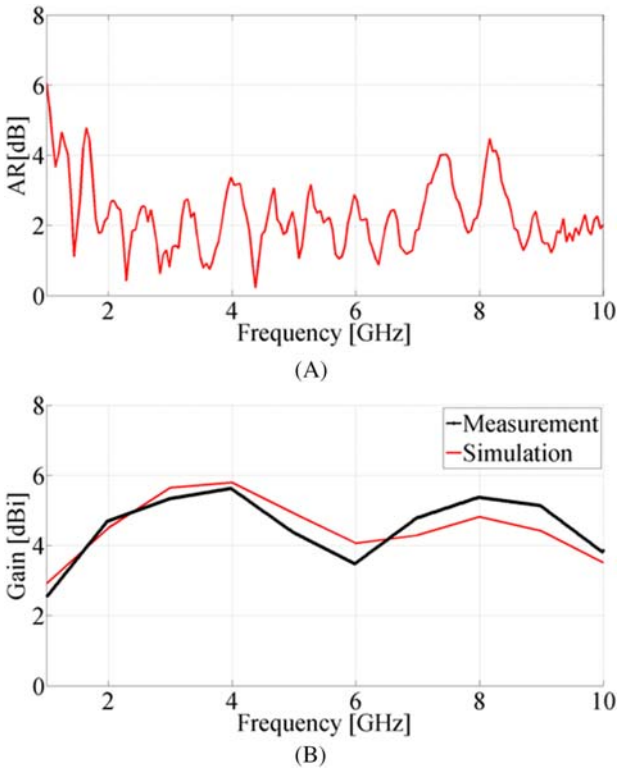

FIGURE 10 (A) Axial ratio measured and simulated of the antenna and (B) measured and simulated gain of the antenna. [Color figure can be viewed at wileyonlinelibrary.com]

4 | EXPERIMENTAL RESULTS

The designed antenna and impedance adapter were implemented and integrated as shown in Figure 7. Different parameters of the antenna-adapter system were measured in order to characterize it and validate the numerical results.

A N9918A network analyzer from Keysigtht with a bandwidth of 26.5 GHz was used to measure the reflection coefficient and subsequently the input impedance. The numerical results and the corresponding measurements are shown in Figure 8. It can be seen that the behavior of both curves is similar and presents small differences around 5 GHz. The measurement shows that the magnitude of the reflection coefficient is kept below −20 dB in almost all the operation range and presents two small regions that reach −16.3 dB around 8.5 and 9.5 GHz, respectively. Figure 9 shows the real and imaginary part of the input impedance of the antenna-adapter system, in (a) and (b), respectively. The real part has an average value of 50 Ω with a maximum deviation of 11 Ω around 9.5 GHz, while the imaginary part of the impedance has an average value of 0 Ω, with a maximum deviation of 16 Ω around 9 GHz. Both high frequency oscillations are related to the practical implementation of the antenna at the origin of the spiral and the connection of the balun/impedance adapter.

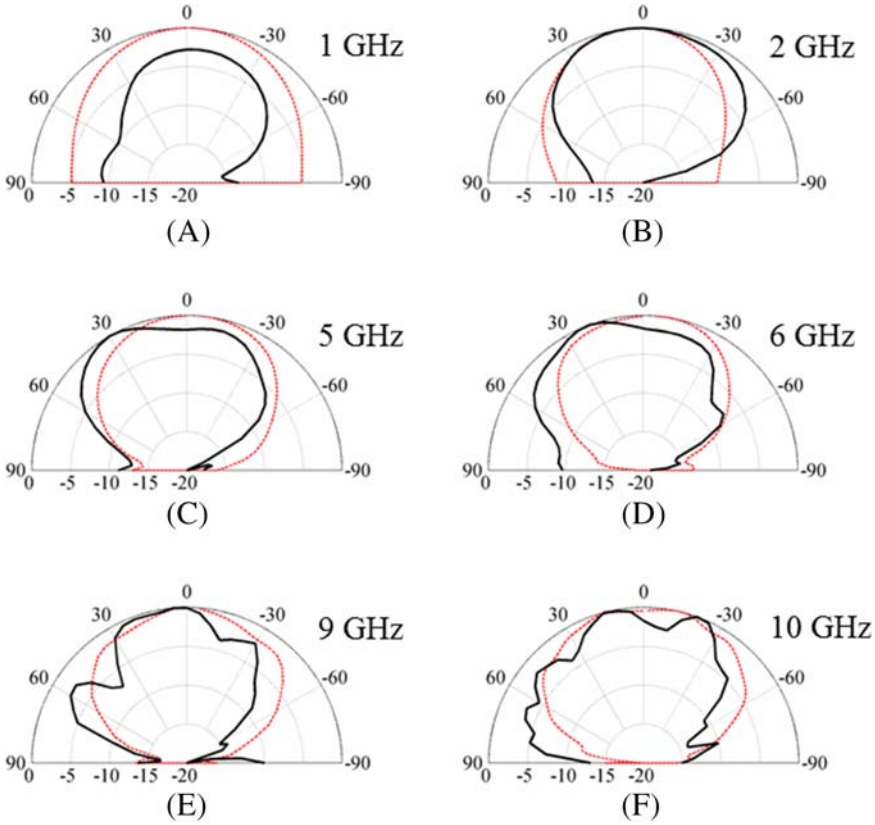

FIGURE 11 Measured (solid line) and simulated (dashed line) radiation pattern averaged over 20 realizations and 72 azimuthal cuts at (A) $f = 1$ GHz, (B) $f = 2$ GHz, (C) $f = 5$ GHz, (D) $f = 6$ GHz, (E) $f = 9$ GHz, and (F) $f = 10$ GHz. [Color figure can be viewed at wileyonlinelibrary.com]

The measured broadside axial ratio (AR), which serves as a means to quantify the quality of the state of polarization of the irradiated wave, is shown in Figure 10A. The method of measurement consists in the implementation of a link using a transmitting antenna with linear polarization, which was rotated in the axial direction, and the designed logarithmic spiral antenna at the receiver end. The vector signal level measured for each rotation angle is produced by averaging 20 realizations that were smoothed with a five samples moving average filter to calculate the axial ratio. As expected, the AR at low frequencies increases due the current reflection at the end of each spiral arm. As the frequency increases, the AR improves, achieving an average value of 2 dB.

To characterize the gain of the antenna-adapter system, the measurement was done with the two antennas method, for which two identical logarithmic spiral antennas and adapters were constructed. Figure 10B shows the measured and simulated gain, where it is possible to observe the similarity between the two curves. The gain values have a maximum of approximately 6 dBi, which are consistent with this kind of planar antenna, as well as the oscillatory behavior that occur due to truncation of the external radius.[19]

Finally measured and simulated radiation pattern of the proposed antenna are shown in Figure 11, where only the broadside is presented. The measurement was obtained averaging 20 realizations over 72 azimuthal cuts. The pattern plotted for 1 GHz, 2 GHz, 5 GHz, 6 GHz, 9 GHz, and 10 GHz show a good agreement between simulations and measurements when the frequency increase. In all cases, the −3 dB beamwidth is approximately 80°, without sidelobes and a highly defined minimum in the end fire side of the antenna. Simulations did not show any adverse effects as alignment errors, for example, being this imperfections the principal discrepancies between measurements and simulation results.

5 | CONCLUSIONS

The design, fabrication and measurement of a logarithmic spiral antenna with the corresponding balun/impedance adapter to operate in the frequency band from 1 to 10 GHz was presented, considering as primary goal to minimize the reflection coefficient. A new method was proposed for the calculation of microstrip lines when a finite ground plane was used. From this analysis the dimensions of the balanced end that allows to obtain a specific impedance was determined. The adapter was modeled in order to consider the effect produced by narrowing both the conducting line and the finite ground plane, on the impedance and consequently, the reflection coefficient. Finally, measurements were performed to characterize the matched antenna and an excellent agreement between measured and simulated results was satisfactorily found. A measured return loss of over 20 dB in most of the frequency range and higher than 16 dB in all of it, exceeds the design requirement and presents an enhancement compared to the results obtained in the specific literature. The gain and the axial ratio of the antenna, were both consistent with the expected values and those presented in similar designs. The proposed method consists in a simple and accurate way to design a balun/adapter for frequency independent planar antennas which not only allows a considerable reduction of the reflection coefficient, but also maintains the broadband characteristic of the implemented antenna.

ACKNOWLEDGMENTS

This work was partially supported by Instituto Balseiro and Consejo Nacional de Investigaciones Científicas y Técnicas (CONICET). The authors are with the Photonics and Microwaves Laboratory of the Instituto Balseiro. LM is researcher of CNEA, PACC and LABR are researchers of CONICET and Universidad Nacional de Cuyo.

REFERENCES

[1] Rumsey V. Frequency independent antennas. *1958 IRE Int Convent Rec*. 1957;5:114–118.

[2] Zhang Y, Brown A. Archimedean and equiangular slot spiral antennas for UWB communications. *Eur Microw. Conf*. Manchester, UK, 2006;1578–1581.

[3] Elmansouri M, Filipovic S. Pulse distortion and mitigation thereof in spiral antenna-based UWB communication systems. *IEEE Trans Antennas Propag*. 2011;59:3863–3871.

[4] Mao S, Yeh J, Chen S. Ultrawidebanda circularly polarized spiral antenna using integrated balun with application to time-domain target detection. *IEEE Trans Antennas Propag*. 2009;57:1914–1920.

[5] Mushiake Y. Self-complementary antennas. *IEEE Antennas Propag Mag*. 1992;34:23–29.

[6] Li MY, Tilley K, McCleary J, Chang K. Broadband coplanar waveguide—coplanar strip—fed spiral antenna. *Electron Lett*. 1955;31:4–5.

[7] Tu W, Li M, Chang K. Broadband microstrip—coplanar stripline—fed circularly polarized spiral antenna. *IEEE Antennas Propag Soc Int Symp*. Albuquerque, NM, 2006;3669–3672.

[8] Wang C, Wu J. A cpw—fed two—arm spiral slot antenna. *Microw Opt Technol Lett*. 2009;51:222–225.

[9] Vinayagamoorthy K, Coetzee J, Jayalath D. Microstrip to parallel strip balun as spiral antenna feed. IEEE 75th Vehicular Technology Conference, 2012, pp. 1–5.

[10] Fu W, Lopez ER, Rowe WST, Ghorbani K. A planar dual arm equiangular spiral antenna. *IEEE Trans Antennas Propag*. 2010; 58:1775–1779.

[11] Chernobrovkin R, Ivanchenko I, Pischikov V, Popenko N. Uwb equiangular spiral antenna for 7.5–40 GHz. *Microw Opt Technol Lett*. 2012;54:2190–2194.

[12] Oh S, Ahn C. Two-arm Archimedean spiral antenna fed by double sided parallel strip line. *Microw Opt Technol Lett*. 2016;58: 1879–1883.

[13] Morbidel L, Bulus L, Costanzo P. Diseño de un agrupamiento de lineal de 8 antenas de banda ancha. XV Reunión de trabajo en procesamiento de la información y control (RPIC), 2013, pp. 503–509.

[14] Morbidel L, Bulus Fiorini LF, Costanzo P. Diseño y medición de una antena espiral logarítmica para aplicaciones de uwb. IEEE Biennial congress of Argentina (ARGENCON), 2016.

[15] Morbidel L, Bulus L, Costanzo P. Adaptador de impedancias para antenas de 9 GHz de ancho de banda. IEEE Biennial Congress of Argentina (ARGENCON), 2014, pp. 612–615.

[16] Svacina J. New method for analysis of microstrip with finite width ground plane. *Microw Opt Technol Lett.* 2006;48:396–399.

[17] Kaiser J. The Archimedean two-wire spiral antenna. *IRE Trans Antennas Propag.* 1960;8:312–323.

[18] Cheng S, Liang Z. The impedance matching analysis on different tapered line functions. *Proc IEEE* 2011;99:620–623.

[19] McFadden M, Scott M. Analysis of the equiangular spiral antenna on a dielectric substrate. *IEEE Trans Antennas Propag.* 2007;55:3163–3171.

How to cite this article: Morbidel L, Bulus Rossini LA, Costanzo Caso PA. Design of high return loss logarithmic spiral antenna. *Microw Opt Technol Lett.* 2017;59:2532–2538. https://doi.org/10.1002/mop.30777

Received:

DOI: 10.1002/mop.30805

Reconfigurable negative group delay circuit with low signal attenuation

Gang Liu | **Jinping Xu**

State Key Laboratory of Millimeter Waves, School of information Science and Engineering, Southeast University, Nanjing 210096, People's Republic of China

Correspondence
Gang Liu, State Key Laboratory of Millimeter Waves, School of information Science and Engineering, Southeast University, Nanjing, 210096, People's Republic of China.
Email: 230129588@seu.edu.cn

Abstract

A novel circuit scheme is presented for the design of reconfigurable negative group delay circuit (RNGDC) with very low signal attenuation (SA), which is based on a lossy coupled-line Microstrip (MS) resonator. Theoretical analysis indicates that reconfigurable characteristics in the proposed circuits can be obtained by tuning the resistance of the variable resistor, which is loaded at a specific point on the MS resonator. Based on the study of one-stage RNGDC, a two-stage RNGDC arranged in an anti-symmetrical manner is designed to provide an extended reconfigurable negative group delay range. To validate the performance of the proposed circuit scheme, the prototypes of one-stage and two-stage RNGDC have been designed working at a center frequency of 1.73 GHz. Measured results of the two-stage RNGDC exhibit a group delays variation of −2 ns to −10 ns with signal attenuation variation of −4.5 dB to −9.3 dB at the center frequency, which demonstrates much lower SA compared to the previously-reported RNGDCs.

KEYWORDS

low signal attenuation, Microstrip resonator, negative group delay (NGD), reconfigurable

1 | INTRODUCTION

Negative group delay (NGD) networks at microwave frequencies have attracted much attention in recent years due to their practical and potential applications in a variety of microwave systems. They have been used to shorten or eliminate delay lines, enhance the efficiency of a feed-forward linear amplifier, and minimize beam-squint in phased array antenna systems. It is noteworthy that most of previous works related to NGDC can provide only a fixed negative group delay.[1–4] To obtain a reconfigurable NGD, the circuits presented in[5–7] realize the RNGDC based on the reflection-type networks. These circuits show the group delays variation of −2 ns to −10 ns with signal attenuation variation of −20 dB to −40 dB at designed center frequency. The major drawback of these circuits is the high signal attenuation, which severely limits the application of the RNGDCs. Meanwhile, the reflection-type networks need a hybrid coupler which will increase the circuit complexity and circuit size. Therefore, the design of compact RNGDC with considerable NGD reconfigurable range while keeping low SA is an attractive topic in microwave engineering practice.

In this letter, a transmission-type RNGDC based on lossy coupled-line MS resonator that is loosely coupled with the main transmission line is presented. This circuit exhibits a compact circuit structure. Simulation work reveals that the proposed transmission-type RNGDC based on the proposed MS resonator can obtain a considerable NGD level while SA keeps on a low level. In order to enhance the reconfigurable range of NGD value, a two-stage reconfigurable NGDC is